Article

Surface Reactivity of the Quinone/Hydroquinone Redox Center Tethered to Gold: Comparison of Delocalized and Saturated Bridges

Scott A Trammell, Martin Moore, Daniel Lowy, and Nikolai Lebedev

J. Am. Chem. Soc., **2008**, 130 (16), 5579-5585 • DOI: 10.1021/ja710246n • Publication Date (Web): 29 March 2008

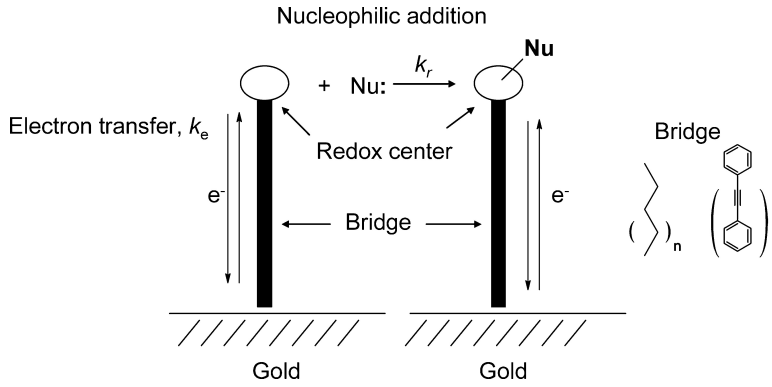

More About This Article

Additional resources and features associated with this article are available within the HTML version:

- Supporting Information
- Links to the 1 articles that cite this article, as of the time of this article download
- Access to high resolution figures
- Links to articles and content related to this article
- Copyright permission to reproduce figures and/or text from this article

View the Full Text HTML

J|A|C|S
ARTICLES

Published on Web 03/29/2008

Surface Reactivity of the Quinone/Hydroquinone Redox Center Tethered to Gold: Comparison of Delocalized and Saturated Bridges

Scott A Trammell,* Martin Moore, Daniel Lowy,† and Nikolai Lebedev

Center for Bio-Molecular Science and Engineering, Naval Research Laboratory, Washington, D.C. 20375, and Nova Research, Inc., 1900 Elkin Street, Alexandria, Virginia 22308

Received November 12, 2007; E-mail: scott.trammell@nrl.navy.mil

Abstract: We found that when a quinone headgroup, present in a mixed self-assembled monolayer on gold, reacts with a nucleophile, dissolved in the bulk phase, the reaction rate widely depends on the chemical nature of the tether, being 7 times faster for quinones attached via a delocalized bridge as compared to a saturated alkane chain. Cyclic voltammetry (CV) of the quinone/hydroquinone redox couple was used to monitor the nucleophilic addition, while simulated CVs compared to experimental runs permitted the determination of rate constants. Analysis of CV data also suggests that the delocalized oligo(phenylene ethynylene) bridge facilitates the addition of two mercaptoethanol molecules as compared to the alkane bridge, where only one molecule is being added. The use of delocalized bridges for tethering quinones to electrodes is of great potential in electrochemically controlled "tuning" of surfaces needed in biosensor applications.

Introduction

Self-assembled monolayers (SAMs) have been employed in numerous surface and electron transfer (ET) studies since they provide structurally well-defined surfaces at modified electrodes.[1–9] A major topic of this work is to understand the role of the bridging group in ET reactions of surface-confined redox centers, contained in the SAM (Figure 1). Since electrons must tunnel through the ET barrier to the electrode surface, the properties of the bridge are essential. For alkanethiols, the ET rate decays exponentially with distance, $k = k_0 \exp(-\beta r)$, where k is the first-order ET rate constant measured at a certain distance r (in Å), while k_0 is the ET rate constant extrapolated to zero distance,[10] and the electron tunneling decay constant, β is in the range of $\sim 0.8-1$ Å^{-1}.[10] Molecules containing delocalized bridges ("molecular wires") such as oligo(phenylene ethynylene) (OPE) or oligo(phenylene vinylene) (OPV) show enhanced electron tunneling, as ferrocene-terminated OPEs are characterized by β values ranging from 0.4 to 0.6,[11,12] while ferrocene-terminated OPVs show distance-independent ET rates up to 28 Å.[13,14]

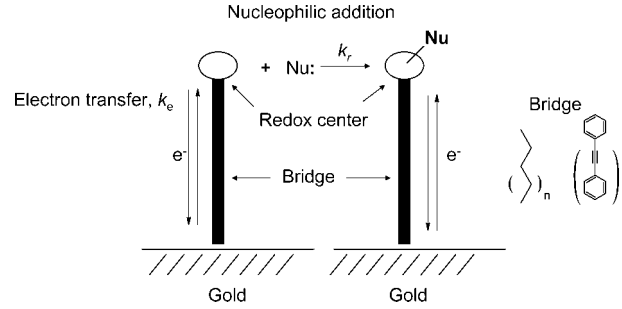

Figure 1. Schematic representation of the different reactions underwent by redox centers contained in SAMs; different bridging groups are highlighted.

To our knowledge, despite the extensive investigations performed on SAMs, the effect of bridging groups on the chemical reactions of redox headgroups with bulk phase species

† Nova Research, Inc.

(1) Finklea, H. O. Electrochemistry of Organized Monolayers of Thiols and Related Molecules on Electrodes. In *Electroanalytical Chemistry*; Bard, A. J. ; Rubinstein, I. , Eds.; Marcel Dekker, Inc.: New York, 1996; Vol. 19, pp 109–335..
(2) Smalley, J. F.; Feldberg, S. W.; Chidsey, C. E. D.; Linford, M. R.; Newton, M. D.; Liu, Y. P. *J. Phys. Chem. B* **1995**, *99*, 13141–13149.
(3) Ravenscroft, M. S.; Finklea, H. O. *J. Phys. Chem. B.* **1994**, *98*, 3843–3850.
(4) Zhang, L. T.; Lu, T. B.; Gokel, G. W.; Kaifer, A. E. *Langmuir* **1993**, *9*, 786–791.
(5) Becka, A. M.; Miller, C. J. *J. Phys. Chem. B* **1992**, *96*, 2657–2668.
(6) Chidsey, C. E. D. *Science* **1991**, *251*, 919–922.
(7) Chidsey, C. E. D.; Bertozzi, C. R.; Putvinski, T. M.; Mujsce, A. M. *J. Am. Chem. Soc.* **1990**, *112*, 4301–4306.
(8) Hong, H. G.; Park, W. *Langmuir* **2001**, *17*, 2485–2492.
(9) Hong, H. G.; Park, W. *Bull. Korean Chem. Soc.* **2005**, *26*, 1885–1888.
(10) Kaifer, A. E.; Gómez-Kaifer, M. *Supramolecular Electrochemistry;* Wiley-VCH: New York, 1999; p 223.
(11) Sachs, S. B.; Dudek, S. P.; Hsung, R. P.; Sita, L. R.; Smalley, J. F.; Newton, M. D.; Feldberg, S. W.; Chidsey, C. E. D. *J. Am. Chem. Soc.* **1997**, *119*, 10563–10564.
(12) Creager, S.; Yu, C. J.; Bamdad, C.; O'Connor, S.; MacLean, T.; Lam, E.; Chong, Y.; Olsen, G. T.; Luo, J.; Gozin, M.; Kayyem, J. F. *J. Am. Chem. Soc.* **1999**, *121*, 1059–1064.
(13) Dudek, S. P.; Sikes, H. D.; Chidsey, C. E. D. *J. Am. Chem. Soc.* **2001**, *123*, 8033–8038.
(14) Sikes, H. D.; Smalley, J. F.; Dudek, S. P.; Cook, A. R.; Newton, M. D.; Chidsey, C. E. D.; Feldberg, S. W. *Science* **2001**, *291*, 1519–1523.

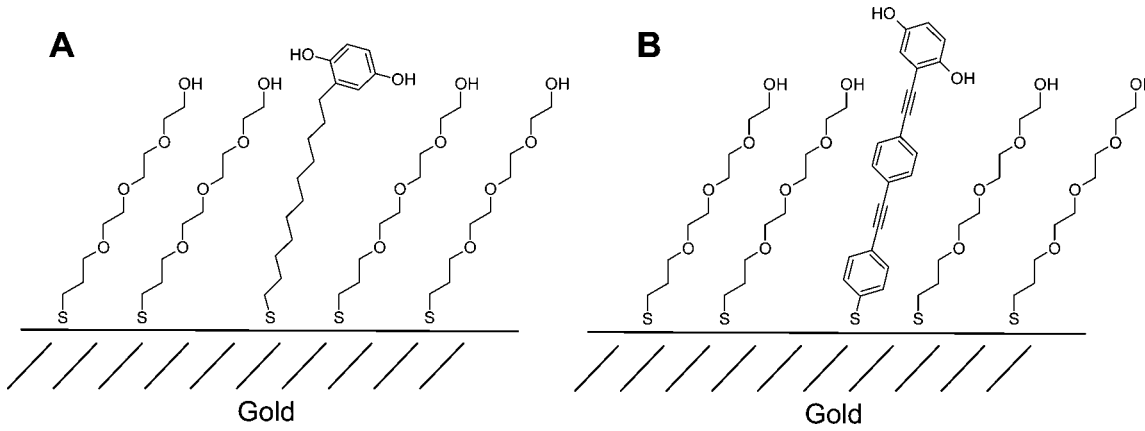

Figure 2. Structures of compounds H_2Q-alkane (A) and H_2Q-OPE (B) in mixed monolayers on gold, using PEG as a diluent.

is still largely unexplored. We previously reported that compounds containing the hydroquinone/quinone (H_2Q/Q) redox headgroup attached via oligo(phenylene vinylene) (OPV) bridges and thiol anchor groups, can form well-ordered SAMs on gold. We also demonstrated the enhanced electron tunneling ability of the delocalized OPV bridge, which increases the rate of the proton-coupled ET reaction of the hydroquinone headgroup, as compared to the ET rate accomplished with a saturated bridge of similar length.[15,16]

In addition to proton-coupled ET, quinones can undergo various chemical reactions, as well.[17] Molecular orbital calculations performed on 1,4-benzoquinone show a very uneven distribution of π-electron density, which accounts for its broad spectrum of activity.[18] For a quinone attached to a chemically modified electrode, several types of its surface reactions can be controlled and monitored electrochemically. Examples include interfacial Diels–Alder reactions,[19,20] additions of alkyl and aryl amines,[21] additions of thiols,[22] and reactions with oxyamine.[23] Most of these examples make use of saturated alkane bridges for attaching the quinone headgroup to the electrode surface.

Given that surface-confined quinones are being employed in surface reactions for tailoring sensing surfaces and controlling cell adhesion,[24,25] an enhancement of the rate of the chemical step would be a valuable asset. Accordingly, the main goal of the present study is to compare the ability of a quinone to react with a nucleophile, when the quinone is tethered to gold using either a delocalized or saturated bridge (Figure 1). By means of cyclic voltammetry monitoring of the surface reaction, we compared the nucleophilic addition of mercaptoethanol to the quinone ring, when it was bridged to the surface via a delocalized (H_2Q-OPE), the control being a saturated (H_2Q-alkane) bridge. In both cases mixed monolayers were assembled on gold electrodes, with a polyethylene glycol alkane thiol (PEG) as a diluent (see Figure 2 for structures of compounds; H_2Q-alkane, H_2Q-OPE, and PEG formed in mixed monolayers on gold).

Experimental Section

Materials. Dichloromethane (DCM), tetrahydrofuran (THF), toluene, ethyl acetate, hexanes, methanol, ethanol, tri(ethylene glycol), allylbromide, azobisisobutyronitrile (AIBN), *N*,*N*′-diisopropylethyl-amine, copper(I) iodide, and bis(triphenylphosphine) palladium(II) dichloride tetrabutylammonium fluoride (1 M, THF), boron tribromide (1 M in DCM) were purchased from Aldrich Chemical Co. 2-Ethynyl-1,4-dimethoxybenzene,[24] [(4-bromophenyl)ethynyl](trimethyl)silane,[25] *S*-(4-iodophenyl)ethanethioate,[26] and 1,4-dihydroxy-2-(11-thioacetate)undecylbenzene (H_2Q-alkane)[19] were synthesized according to previously reported protocols.

Prop-1-en-3yltri(ethylene glycol). A solution of 50 wt % sodium hydroxide in water (6.5 mL, 82 mmol) was added to tri(ethylene glycol) (62.1 g, 413 mmol) in a 500 mL flask and heated to 100 °C, while stirring for 30 min under nitrogen. Next, allyl bromide (10 g, 82 mmol) was added to the reaction, and stirred overnight at 100 °C. After which, the reaction mixture was cooled and extracted multiple times with hexane. Hexane extractions were combined and rotary evaporated to give yellow oil. The oil was then purified by chromatography on silica gel using ethyl acetate (3.0 g, 20% yield). ^{1}H NMR ($CDCl_3$): δ 3.11(s, 1H), 3.53–3.67 (m, 12H), 3.97–3.95 (t, 2H), 5.10–5.23 (dd, 2H), 5.61–5.88 (m, 1H).

[1-[(Methylcarbonyl)thio]prop-3-yl]tri(ethylene glycol). Prop-1-en-3yltri(ethylene glycol (3.0 g, 15.8 mmol) and AIBN (400 mg, catalyst) were dissolved in toluene (40 mL). Next, thiol acetic acid (2.5 g, 31.4 mmol) was added and heated to reflux overnight. After the reaction mixture cooled, the solvent was removed by rotary evaporation to give yellow oil. The oil was then purified by chromatography on silica gel using ethyl acetate (1.5 g, 36% yield).^{1}H NMR ($CDCl_3$): δ 1.79–1.83 (m, 2H), 2.28 (s, 3H), 2.88–2.92 (t, 2H), 3.45–3.48 (t, 2H), 3.53–3.68 (m, 12H).

(1-Mercaptoprop-3-yl)tri(ethylene glycol) (PEG). [1-[(Methylcarbonyl)thio]hex-6-yl]tri(ethylene glycol) (1.5 g, 5.6 mmol) was added under nitrogen atmosphere to a 300 mL flask containing 0.1 M HCl in methanol. The reaction mixture was refluxed overnight and cooled, and the solvent was removed by rotary evaporation to give light-yellow oil. The oil was then purified by chromatography

(15) Trammell, S. A.; Lowy, D. A.; Seferos, D. S.; Moore, M.; Bazan, G. C.; Lebedev, N. *J. Electroanal. Chem.* **2007**, *606*, 33–38.
(16) Trammell, S. A.; Seferos, D. S.; Moore, M.; Lowy, D. A.; Bazan, G. C.; Kushmerick, J. G.; Lebedev, N. *Langmuir* **2007**, *23*, 942–948.
(17) Patai, S. *The Chemistry of the Quinonoid Compounds;* Interscience: New York, London, 1974.
(18) Kutyrev, A. A. *Tetrahedron* **1991**, *47*, 8043–8065.
(19) Kwon, Y.; Mrksich, M. *J. Am. Chem. Soc.* **2002**, *124*, 806–812.
(20) Bunimovich, Y. L.; Ge, G. L.; Beverly, K. C.; Ries, R. S.; Hood, L.; Heath, J. R. *Langmuir* **2004**, *20*, 10630–10638.
(21) Katz, E. *J. Electroanal. Chem.* **1992**, *326*, 197–212.
(22) Curreli, M.; Li, C.; Sun, Y. H.; Lei, B.; Gundersen, M. A.; Thompson, M. E.; Zhou, C. W. *J. Am. Chem. Soc.* **2005**, *127*, 6922–6923.
(23) Chan, E. W. L.; Yousaf, M. N. *J. Am. Chem. Soc.* **2006**, *128*, 15542–15546.
(24) Mu, F. R.; Hamel, E.; Lee, D. J.; Pryor, D. E.; Cushman, M. *J. Med. Chem.* **2003**, *46*, 1670–1682.
(25) Yu, C. J.; Chong, Y.; Kayyem, J. F.; Gozin, M *J. Org. Chem.* **1999**, *64*, 2070–2079.
(26) Hsung, R. P.; Babcock, J. R.; Chidsey, C. E. D.; Sita, L. R. *Tetrahedron Lett.* **1995**, *36*, 4525–4528.

on silica gel using ethyl acetate (500 mg, 14% yield). ^{1}H NMR ($CDCl_3$): δ 1.79–1.83 (m, 2H), 2.57–2.58 (t, 2H), 3.47–3.72(m, 14H).

({4-[(2,5-Dimethoxypheny)ethynyl]phenyl}ethynyl)(trimethyl) silane (1). In a 150 mL pressure flask equipped with a Teflon-coated magnetic stir bar, were disssolved 2-ethynyl-1,4-dimethoxybenzene (4.88 g, 30.1 mmol), [(4-bromophenyl)ethynyl](trimethyl)silane (7.7 g 30 mmol), bis(triphenylphosphine)−palladium(II) dichloride (0.4 g, 0.56 mmol), and copper(I) iodide (0.05 g, 0.26 mmol) under nitrogen in a mixture of THF (30 mL) and diisopropylehtylanime (30 mL), and then the flask was sealed. The reaction was stirred for 48 h at 60 °C. The mixture was then cooled to room temperature, and filtered through a plug of silica gel with 1:1 hexane/ethyl acetate. The organic solvent was removed by rotary evaporation to give a dark crude product. Chromatography on silica gel eluting with 4:1 hexane/ethyl acetate to yield a solid (4.64 g, 44.8% yield). ^{1}H NMR ($CDCl_3$): δ 7.53 (d, 2H), 7.47 (d, 2H), 7.07 (s, 1H), 6.90–6.85 (m, 2H), 3.90 (s, 3H), 3.80 (s, 3H), 0.0 (s, 9H). MS *m*/*z*: M^+ 334.

2-[(4-Ethynylphenyl)ethynyl]-1,4-dimethoxybenzene (2). In a 250 mL round-bottom flask equipped with a Teflon-coated magnetic stir bar, tetrabutylammonium fluoride 1.0 M in THF (14.0 mL, 14 mmol) was added dropwise to **1** (3.79 g, 11.3 mmol) in THF (50 mL) and water (5 mL) at 0 °C, under nitrogen atmosphere, with constant stirring. The reaction was stirred at 0 °C for 1 h, and then at room temperature for 3 h. The reaction was quenched with water and extracted with ethyl acetate. Chromatography on silica gel eluting with 4:1 hexane/ethyl acetate, yielded a dark-yellow solid (2.02 g, 75% yield). ^{1}H NMR ($CDCl_3$) δ 7.55 (d, 2H), 7.50 (d, 2H), 7.07 (s, 1H), 6.90–6.85 (m, 2H), 3.91 (s, 3H), 3.82 (s, 3H), 3.20 (s, 1H). MS *m*/*z*: M^+ 234.

S-[4-(2-{−4-[2-(2,5-Dimethoxyphenyl)ethynyl]phenyl}ethynyl)-phenyl]ethanethioate (3). In a 150 mL pressure flask with a Teflon-coated magnetic stir bar, were dissolved compound **2** (1.87 g, 7.13 mmol), *S*-4-iodophenyl)ethanethioate (1.98 g, 7.13 mmol), bis-(triphenylphosphine)palladium(II) dichloride (0.15 g, 0.21 mmol), and copper(I) iodide (0.01 g, 0.05 mmol) in a mixture of THF (15 mL) and diisopropylehtylanime (15 mL) with nitrogen, and then the flask was sealed. The reaction was stirred for 48 h at 60 °C. After that the mixture was cooled to room temperature and filtered through a plug of silica gel with 1:1 hexane/ethyl acetate. The organic solvent was removed by rotary evaporation to give a dark crude product. Chromatography on silica gel eluting with 4:1 hexane/ethyl acetate yielded a solid (1.5 g, 51% yield). ^{1}H NMR ($CDCl_3$) δ 7.59–7.50 (m, 6H), 7.44 (d, 2H), 7.07 (s, 1H), 6.90–6.86 (m, 2H), 3.91 (s, 3H), 3.82 (s, 3H), 2.47 (s, 3H). MS *m*/*z*: M^+ 412.

***S*-[4-(2-{4-[2-(2,5-Dihydroxyphenyl)ethynyl]phenyl}ethynyl)-phenyl]ethanethioate, (H_2Q-OPE).** In a 25 mL round-bottom flask, equipped with a Teflon-coated magnetic stir bar, boron tribromide 1 M in DCM (1 mL) was added dropwise to 100 mg of **3** in 5 mL of DCM, at –78 °C, under nitrogen atmosphere, with constant stirring. The mixture was allowed to warm to room temperature. After 30 min, the reaction was cooled down to 0 °C, and 5 mL of cold water was added. The solution was permitted to warm to room temperature. After 30 min, the mixture was diluted with 50 mL of ethyl acetate and 50 mL of aqueous 4 M NaCl. After the organic phase was separated, the solvent was removed by rotoevaporation. Chromatography on silica gel eluting with 1:1 hexane/ethyl acetate yielded a yellow solid. The solid was redissolved in 2 mL of DCM and added to 50 mL of hexanes. A pale-yellow precipitate was collect by vacuum filtration (10 mg, 10.7% Yield). ^{1}H NMR (acetone-d_6) δ 8.22 (s, 1H), 7.97 (d, ^{3}J = 11.62 Hz, 2H), 7.7–7.6 (m, 4H), 7.51 (d, ^{3}J = 8.29 Hz, 2H), 7.4 (d, 1H), 7.302 (s, 1H) 7.07 (d, ^{4}J = 2.27 Hz 1H), 6.89 (dd, 1H), 2.45 (s, 3H). MS *m*/*z*: M^+ 384

Monolayer Deposition on Gold Coil Electrodes. Gold coil working electrodes were made in-house according to a previously described procedure.[27] For electrochemical measurements the coiled end of each working electrode was submersed in electrolyte (2 mL), and the exposed uncoiled end was connected directly to the working electrode lead of the potentiostat. Immersed geometric areas of working electrodes were typically 1.0 ± 0.1 cm^2. Each gold coil electrode was individually cleaned for 30 s in piranha solution. (H_2O_2 + H_2SO_4, 1:3 v/v. **Precaution!** Piranha solution is extremely oxidizing; it must be handled and used under the hood, while continuously wearing eye protection and gloves.) Then, the gold coils were activated electrochemically in 0.1 M H_2SO_4 solution.[27] The cleanliness of the surface was assessed by cyclic voltammetry, in the potential range of 0.0 and 1.5 V vs Ag/AgCl, 3 M KCl, at 200 mV/s (performed in fresh 0.1 M H_2SO_4). Clean gold substrates were modified with SAMs by immersion in 1 mM solution of 1:1 H_2Q-OPE and PEG or 1:1 H_2Q-alkane and PEG, in slightly acidified EtOH, for several hours at room temperature, and then rinsed with copious amounts of ethanol and DI water.

Electrochemistry. All electrochemical measurements were performed in a Faraday cage, in the three-electrode geometry, using a gold coil working electrode, a Pt counter electrode (Bioanalytical Systems, Inc., BAS, West Lafayette, IN), and a Ag/AgCl, 3 M KCl reference (BAS). A 3 mL glass cell (CH Instruments) was utilized, and measurements were driven by an electrochemical workstation (Model 660a, CH Instruments, Austin, TX). Cyclic voltammograms were acquired at room temperature under ambient conditions, without purging the supporting electrolyte with inert gas. Each voltammogram was initiated at the negative potential limit following a 2 s quiescence period.

Electrochemical Simulations. Cyclic voltammograms were simulated with the software supplied by CH Instruments. The 2-electron transfer step for each hydroquinone/quinone redox couple was simulated by assuming an EE mechanism, and keeping for both steps an identical electron transfer coefficient, α, formal potential, $E^{o\prime}$, and electron transfer rate constant, k_e. For the purpose of this work, we believe these assumptions are reasonable. In fact, since the formal potentials of each 1-electron step are close, the voltammetry of the quinone/hydroquinone redox couple in buffered solutions displays one single CV wave.[28]

Modeling of CVs that report on the surface reaction was as follows. For model 1, the reactant and product CVs were simulated and compared to the real CVs for extracting the non-Faradaic capacitance, surface coverage (Γ, mol/cm^2), E_1 and E_2, α, and rate constants of the electron transfer steps, k_{e1} and k_{e2}. To model the surface reaction, k_r (rate constant of the chemical step, see scheme of model 1) was manually adjusted until the percent changes in the anodic peak currents (for both reactant and product) vs scan number became a close match between the simulation and data. For model 2, a similar procedure was applied. Again, the reactant and final product CVs were simulated and compared to the real CVs for deriving non-Faradaic capacitance, surface coverage, E_1 and E_3, α, and rate constants of electron transfer steps, k_{e1} and k_{e3}. In this case in order to model the surface reaction, k_{r1}, k_{r2}, and E_2 were varied manually in the simulation, until the percent changes in both the anodic and cathodic peak currents (for reactant, intermediate, and product) vs scan number were a close match between the data and simulation.

In order to test the consistency of the model, we varied the anodic switching potential between 0.2 and 0.3 V vs Ag/AgCl, and measured the reaction of H_2Q-OPE in the SAM with 1 μM mercaptoethanol in solution. The small variation of k_{r1} and k_{r2} vs anodic switching potential was well within experimental error (see Supporting Information), suggesting that the simulation accounted adequately for the time the H_2Q-OPE SAM spent in the oxidized (reactive) state.

(27) Jhaveri, S. D.; Trammell, S. A.; Lowy, D. A.; Tender, L. M. *J. Am. Chem. Soc.* **2004**, *126*, 6540–6541.
(28) Quan, M.; Sanchez, D.; Wasylkiw, M. F.; Smith, D. K. *J. Am. Chem. Soc.* **2007**, *129*, 12847–12856.

Model 1.

$$A - 2e \leftrightarrows B \qquad E_1, k_{e1}, \alpha \qquad (1)$$

$$B \rightarrow C \qquad k_{r1} \qquad (2)$$

$$C - 2e \leftrightarrows D \qquad E_2, k_{e2}, \alpha \qquad (3)$$

Model 2.

$$A - 2e \leftrightarrows B \qquad (4)$$

$$B \rightarrow C \qquad (5)$$

$$C - 2e \leftrightarrows D \qquad (6)$$

$$D \rightarrow E \qquad (7)$$

$$E - 2e \leftrightarrows F \qquad (8)$$

Results

Surfaces with low coverage in hydroquinone/quinone redox centers were prepared by using PEG as diluent, exposing clean gold electrodes to 1:1 mixtures of 1 mM solutions with a free PEG thiol and either H_2Q-alkane or H_2Q-OPE, having a protected thiol anchor (thiol acetate). Several examples are known for thiol acetate-terminated organic molecules reacting with the gold surface.[16,29–32] When allowed to react with gold, molecules containing thiol acetate yield a structure of the adsorbed species indistinguishable from that obtained with the corresponding free thiols.[33]

After deposition of the mixed SAMs, the surfaces were characterized by cyclic voltammetry performed in 100 mM potassium phosphate buffer at pH 7. Coverage for both H_2Q/Q redox centers were estimated by integrating the anodic and cathodic peaks. For mixed monolayers of H_2Q-OPE/PEG, we found a coverage equaling $\sim 2 \times 10^{-12}$ mol/cm^2 and for H_2Q-alkane/PEG a coverage equaling $\sim 3.5 \times 10^{-12}$ mol/cm^2. CVs of both diluted monolayers showed nearly ideal voltammograms comparable to the simulated curves, providing clear evidence that interactions between the hydroquinone/quinone headgroups were minimized (Figures 3A and 4A).

At a scan rate of 200 mV/s, the measured CVs for the H_2Q-alkane/PEG monolayer displayed highly nonsymmetrical voltammograms with large peak-to-peak separations between the anodic and cathodic peaks (560 mV). Both results are consistent with slow ET rates and $\alpha > 0.5$. Simulated CV with $E = 0.04$ V vs Ag/AgCl, $k = 0.05$ s^{-1}, and $\alpha \approx 0.7$ match well the measured CVs (see Figure 3A). By contrast, CVs of the H_2Q-OPE/PEG monolayer, measured at the same scan rate, displayed reversible electrochemistry, i.e., small peak-to-peak separation (<20 mV), the voltammograms being highly symmetrical. Simulated CVs are a very close match with $E = 0.09$ V vs Ag/AgCl, $k = 35$ s^{-1}, and $\alpha = 0.5$ (Figure 4A). These results are consistent with our previous work for the H_2Q/Q redox center, when comparing OPV and alkane bridges. In those reports, the OPV bridge significantly enhanced the measured rate of the proton-coupled ET of the H_2Q/Q redox center, as compared to the alkane bridge. The explanation resides in the increased tunneling efficiency of the bridge.[15,16]

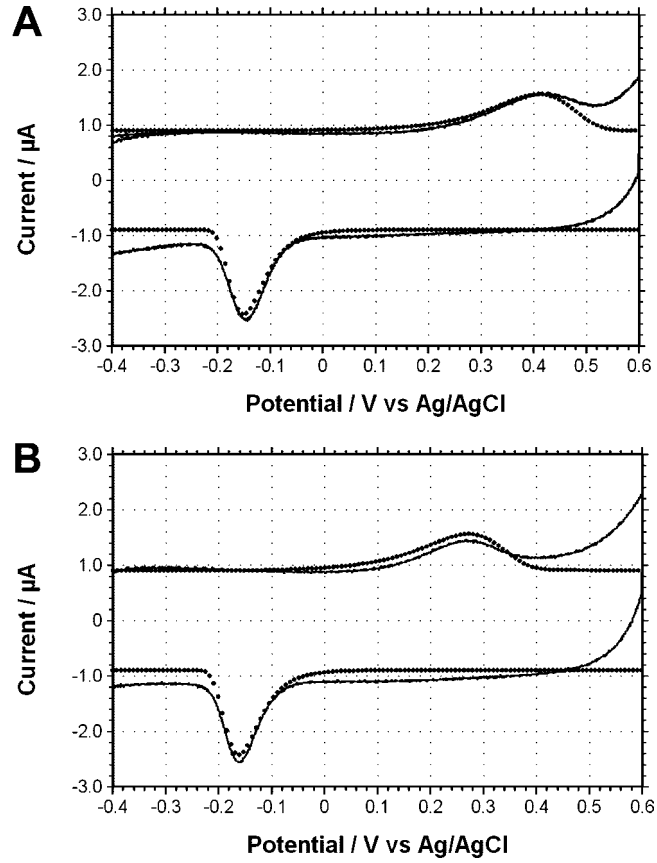

Figure 3. (A) Cyclic voltammograms of a mixed monolayer of H_2Q-alkane and PEG compared to the simulated CV (dotted line) on a gold coil working electrode (in 100 mM potassium phosphate, at pH 7). Scan rate = 200 mV/s. Simulation parameters: $E_1 = 0.04$ V vs Ag/AgCl, $k_{e1} = 0.05$ s^{-1}, $\alpha = 0.7$, coverage ($\Gamma = 3.5 \times 10^{-12}$ mol/cm^2, capacitance = 4.5 μF, and electrode area = 1 cm^2. (B) Cyclic voltammograms after reaction with 1 μM mercaptoethanol compared to a simulated CV (dotted line). Simulation parameters: $E_2 = -0.01$ V vs Ag/AgCl, $k_{e2} = 0.14$ s^{-1}. Coverage, capacitance, electrode area, and α are the same as in (A).

Thiol Reactions. To evaluate the surface reaction of the quinone headgroups in the mixed monolayer, we designed CV experiments that would cycle between the hydroquinone, which is unreactive, through the quinone, which is reactive to thiols. Cyclic voltammograms were recorded at a scan rate appropriate for monitoring the course of reaction, at a given thiol concentration. We found for 2-mercaptoethanol that solutions between 0.5 to 2 μM, at scan rate of 200 mV/s, with 25 scans, were adequate for recording the surface reaction and monitoring it as a function of time. Since the thiol concentration in the bulk phase is in excess and does not change significantly within the course of the reaction, we can consider the surface quinone−bulk phase thiol reaction to be pseudo-first order.

The CV corresponding to the end product of the reaction with 2-mercaptoethanol of the mixed monolayer that contains H_2Q-alkane and PEG is shown in Figure 3B (at pH 7). When compared to the original CV, taken prior to the reaction with thiol, there is a –50 mV shift in formal potential from $E_1 = 0.04$ to $E_2 = -0.01$ V vs Ag/AgCl, along with an increase in ET rate constant, k_e, from 0.05 s^{-1} to 0.14 s^{-1}. Since there is little change in electroactive surface coverage and capacitance, one can state that the PEG diluent is sufficient at blocking the direct reaction of bulk phase thiol with the gold surface. Cyclic

(29) Seferos, D. S.; Banach, D. A.; Alcantar, N. A.; Israelachvili, J. N.; Bazan, G. C. *J. Org. Chem.* **2004**, *69*, 1110–1119.
(30) Wasserman, S. R.; Biebuyck, H.; Whitesides, G. M. *J. Mater. Res.* **1989**, *4*, 886–891.
(31) Skulason, H.; Frisbie, C. D. *J. Am. Chem. Soc.* **2000**, *122*, 9750–9760.
(32) Gryko, D. T.; Clausen, C.; Lindsey, J. S. *J. Org. Chem.* **1999**, *64*, 8635–8647.
(33) Tour, J. M.; Jones Ii, L.; Pearson, D. L.; Lamba, J. J. S.; Burgin, T. P.; Whitesides, G. M.; Allara, D. L.; Parikh, A. N.; Atre, S. V. *J. Am. Chem. Soc.* **1995**, *117*, 9529–9534.

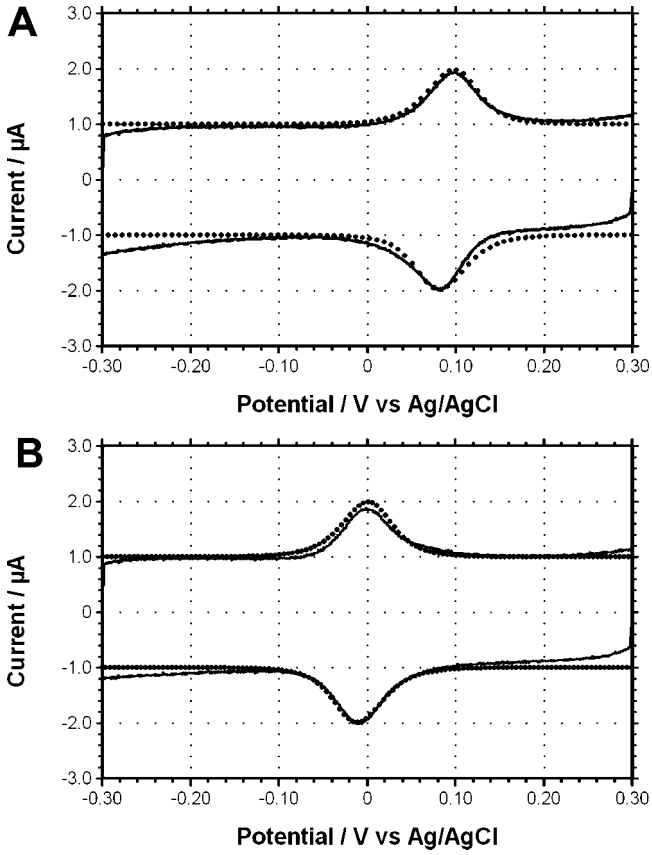

Figure 4. (A) Cyclic voltammograms of a mixed monolayer of H_2Q-OPE and PEG compared to the simulated CV (dotted line) on a gold coil working electrode. Simulation parameters: $E_1 = 0.09$ V vs Ag/AgCl, $k_{e1} = 35\ s^{-1}$, $\alpha = 0.5$, $\Gamma = 2 \times 10^{-12}$ mol/cm^2, capacitance = 5 μF, and electrode area = 1 cm^2. (B) Cyclic voltammograms after reaction with 1 μM mercaptoethanol compared to the simulated CV (dotted line). Simulation parameters: $E_3 = -0.005$ V vs Ag/AgCl, $k_{e3} = 50\ s^{-1}$. Coverage, capacitance, electrode area, and α are the same as in (A).

voltammograms recorded over the course of the reaction exhibit two pseudo isosbestic points at 0.33 V and –0.15 V vs Ag/AgCl, suggesting that the reaction is a two state conversion (Figure 5A). Conversion of the original redox center can be monitored at $E_p = 0.42$ V vs Ag/AgCl, along with a new redox center appearing at $E_p = 0.27$ V vs Ag/AgCl. To extract the pseudo first order rate constant for the surface quinone - bulk phase thiol reaction we simulated the CVs (Figure 5B) according to model 1, as described in the experimental section. A good match was found between the change in peak currents, when comparing data with simulation having $k_r = 0.038\ s^{-1}$ for the chemical reaction step (Figure 5C).

In Figure 4B we display the CV of the end product of the reaction of the mixed monolayer containing H_2Q-OPE and PEG. There is a shift of –95 mV in formal potential from the initial redox center ($E_1 = 0.09$ V vs Ag/AgCl) to the final product ($E_3 = -0.005$ V vs Ag/AgCl). Again, there is little change in surface coverage and capacitance, suggesting that the PEG diluent is sufficient at blocking the reaction of mercaptoethanol, present in the buffer, with the gold surface. Consecutive CV scans, while monitoring the reaction, are shown in Figure 6A. As the scans cycle through the reactive state of quinone, loss of the original redox center is evidenced at $E_{pa} = 0.097$ and $E_{pc} = 0.082$ V vs Ag/AgCl (Figure 6C). In this case, however, there are no pseudo-isosbestic points in the CVs recorded as the reaction proceeds over time. In fact, an intermediate is detected as the

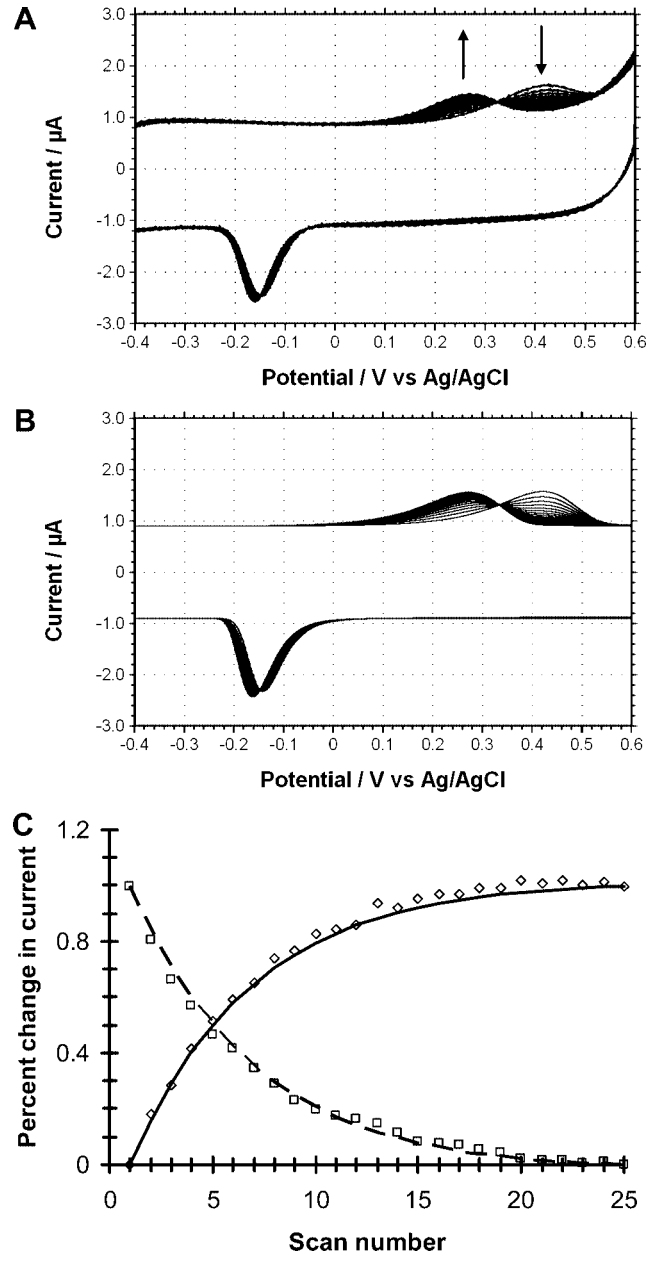

Figure 5. (A) Cyclic voltammograms of a mixed monolayer of H_2Q-alkane and PEG on a gold coil working electrode with the addition of 1 μM mercaptoethanol to the buffer. Scan rate = 200 mV/s. Number of scans = 25. (B) Simulated cyclic voltammograms using model 1 as described in the Experimental Section. Parameters: $k_r = 0.038\ s^{-1}$. All other parameters are the same as in Figure 1B. (C) Percent change of the anodic peak currents for the reactant (□) and product (◇) vs scan number comparing the data with the simulation.

reaction advances to the final product. Formation and decay of the intermediate can be measured at $E_{pa} = 0.049$ and $E_{pc} = 0.035$ V vs Ag/AgCl, along with the formation of the product at $E_{pa} = -0.009$ and $E_{pc} = -0.001$ V vs Ag/AgCl (Figure 6D). In order to extract the pseudo first order rate constants for the reaction of surface quinone — bulk phase mercaptoethanol, we simulated the CVs as described in the experimental section, using model 2 (Figure 6B). A good match was found between the data and simulation, when assuming $k_{r1} = 0.28\ s^{-1}$ and $k_{r2} = 0.05\ s^{-1}$ at $E_2 = -0.04$ V vs Ag/AgCl (Figure 6C and 6D).

To estimate the second-order rate constant for the reaction between the surface quinone and mercaptoethanol in solution, we performed experiments at different concentrations of mer-

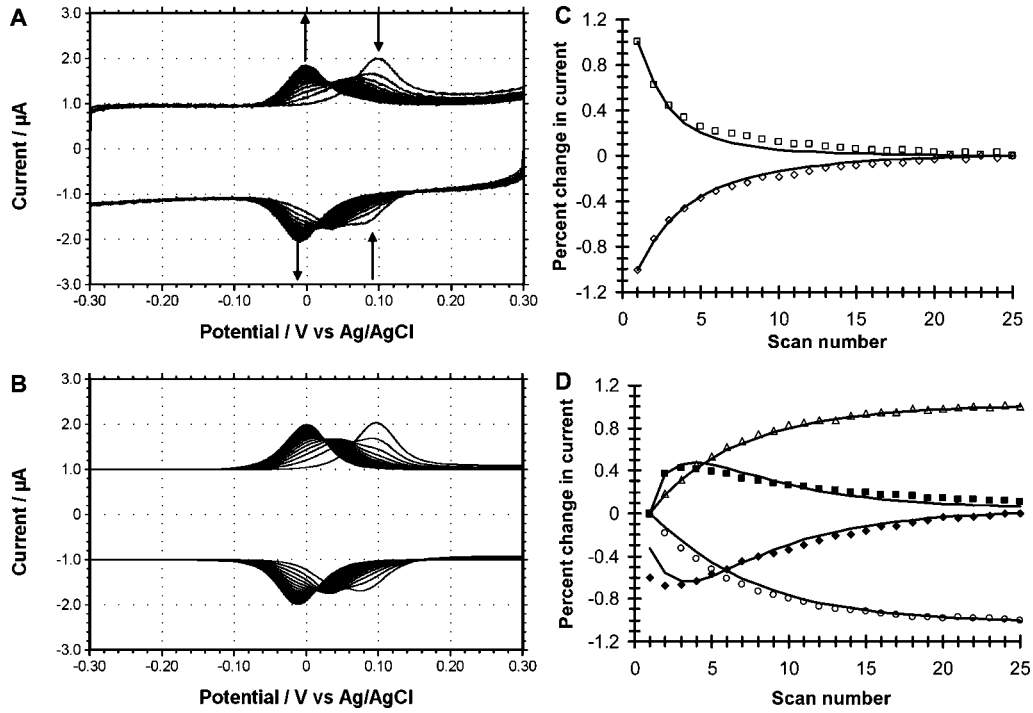

Figure 6. (A) Cyclic voltammograms of a mixed monolayer of H_2Q-OPE and PEG on a gold coil working electrode with the addition of 1 μM mercaptoethanol to the buffer (100 mM potassium phosphate at pH 7). Scan rate = 200 mV/s. Number of scan = 25. (B) Simulated cyclic voltammograms using model 2 as described in the experimental. Parameters: $k_{r1} = 0.28\ s^{-1}$, $E_2 = -0.04$ V vs Ag/AgCl, $k_{e2} = 50\ s^{-1}$, $k_{r2} = 0.05\ s^{-1}$. All other parameters are the same as in Figure 2B. (C) Percent change of both anodic (□) and cathodic (◇) peak currents for the reactant vs scan number comparing the data with the simulation (solid line). (D) Percent change for both the intermediate's anodic (■) and cathodic (◆) peak currents and final product's anodic (△) and cathodic (○) peak currents vs scan number comparing the data with the simulation (solid line).

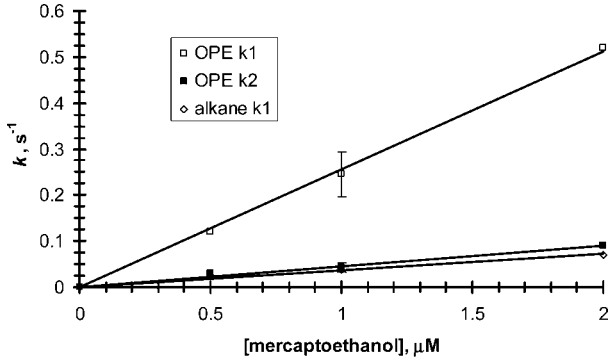

Figure 7. Rate constants extracted from the simulation of the surface reaction of the quinone with mercaptoethanol vs mercaptoethanol concentration.

captoethanol. Both mixed monolayers displayed a linear increase in the observed rate constant with an increase in mercaptoethanol concentration (see Figure 7). The slope of each linear relationship gives the second-order rate constant, as shown by eqs 9–11.

$$\text{Rate}(\text{molcm}^{-2}\ \text{s}^{-1}) = k(\text{M}^{-1}\ \text{s}^{-1})[\text{thiol}]\Gamma_Q(\text{mol/cm}^2) \quad [\text{thiol}] >> \Gamma_Q \tag{9}$$

$$\text{Rate}(\text{molcm}^{-2}\text{s}^{-1}) = k\ (\text{s}^{-1})\Gamma_Q(\text{mol/cm}^2) \tag{10}$$

$$k(\text{s}^{-1}) = k(\text{M}^{-1}\ \text{s}^{-1})[\text{thiol}] \tag{11}$$

The second-order rate constant for first step for the H_2Q-OPE data is $k_{1OPE} = 2.6 \times 10^5\ M^{-1}\ s^{-1}$ and for the second step it is $k_{2OPE} = 0.47 \times 10^5\ M^{-1}\ s^{-1}$. For the H_2Q-alkane data one has $k = 0.36 \times 10^5\ M^{-1}\ s^{-1}$.

Discussion

For quinone groups confined to the surface by either alkane or OPE bridges, there is a negative shift in formal potential, from the initial state to the final product, when bulk phase mercaptoethanol reacts with the quinone headgroup. This finding is consistent with previous reports in which the addition of donating groups shift the formal potential to more negative values, making the hydroquinone state easier to oxidize and the quinone state more difficult to reduce.[21] For the OPE bridge, the shift is nearly twice that of the alkane bridge, i.e., –50 mV as compared to –95 mV. The stepwise shifts from reactant to intermediate, and then to the product, along with the increase of both rate constants with mercaptoethanol concentration in each chemical step, provide strong evidence that the intermediate for the OPE bridge is obtained by single nucleophilic addition of mercaptoethanol, which reacts for a second time at a lower rate to yield the final dithiol product (Figure 8).

The change in rate constant for the proton-coupled electron transfer reaction for both H_2Q-alkane and H_2Q-OPE with the addition of mercaptoethanol is not surprising, since the addition of a donating group (the mercaptan) would change the electronic structure of the molecule's headgroup. Based on resonance structures of the addition product of mercaptan to the ring, two possible mechanisms may account for the increase in rate for the proton-coupled ET reaction at the electrode.

First, the addition of the mercaptan to the ring may change the mechanism of proton-coupled ET. Lavion's analysis using a nine-membered square scheme describes the single proton-

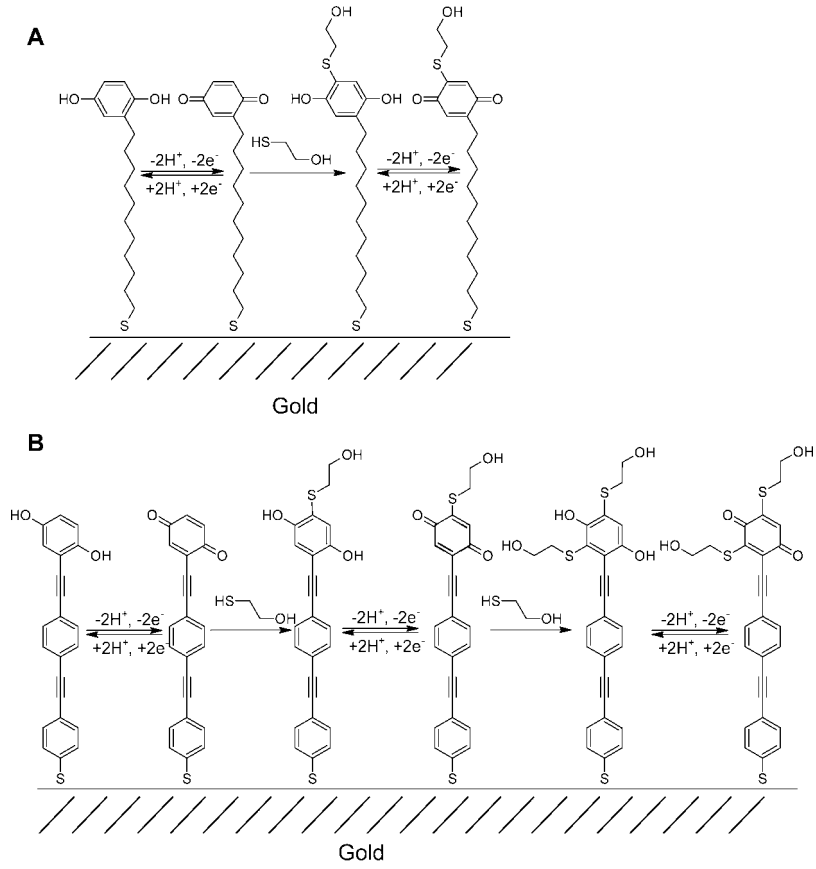

Figure 8. Proposed mechanisms for electrochemically controlled surface reactions of H_2Q-alkane (A) and H_2Q-OPE (B).

and electron-transfer events making up the overall conversion.[34] The order of the steps depends on the pK_a values and the pH of the solution. The addition of the mercaptan may change the pK_a values, which alters the order of events, resulting in an increase in the measured overall rate. Second, based on a Marcus formalism,[35] with the addition of mercaptan there may be a smaller inner sphere reorganizational energy (i.e., smaller changes in bond lengths between the oxidized the reduced states), which would accelerate the ET.

The increase in rate by a factor of 7 for the addition of the first mercaptoethanol molecule to the quinone headgroup, attached by an OPE bridge, as compared to the alkane bridge, is consistent with the known trends of increased rates of nucleophilic addition with delocalization of the electrophile.[36] So far, the exact location of the addition products on the quinone ring is speculative; however, substituent effects on 1,4-quinones were reported to yield 2,5-isomers for donor groups, and 2,3-isomers for acceptor groups.[18]

In conclusion, the reaction of a quinone headgroup in a SAM on gold with a nucleophile in the bulk phase widely depends on the chemical nature of the tether, being much faster when the quinone is attached via a delocalized bridge, as compared to a saturated alkane chain. The nucleophilic addition of mercaptoethanol to quinone headgroups in mixed monolayers on gold was conveniently evaluated by electrochemical techniques, providing insight into the subsistent effects exerted on the quinone ring by the bridging group. The electron-withdrawing effect put forth by the delocalized OPE bridge significantly increased the rate of reaction in the addition of the first mercaptoethanol molecule to the quinone headgroup, as compared to quinones tethered to gold with the alkane bridge. Consequently, the use of delocalized bridges should be advantageous when tethering quinones to electrodes for the electrochemically controlled "tuning" of surfaces in biosensor applications.

Acknowledgment. The support of this work by the Office of Naval Research through a Navy base program at the Naval Research Laboratory Nanoscience Institute is gratefully acknowledged.

Supporting Information Available: NMR spectra of H_2Q-OPE; rate constants estimated from the simulation of the surface reaction of the quinone with mercaptoethanol vs switching potential. This material is available free of charge via the Internet at http://pubs.acs.org.

JA710246N

(34) Laviron, E. *J. Electroanal. Chem.* **1983**, *146*, 15–36.
(35) Marcus, R. A.; Sutin, N. *Biochim. Biophys. Acta* **1985**, *811*, 265–322.
(36) Chattaraj, P. K.; Sarkar, U.; Roy, D. R. *Chem. Rev.* **2006**, *106*, 2065–2091.